



# Phase-sensitive surface X-ray scattering study of a crystalline organic–organic heterostructure

F. Schreiber<sup>a,b,\*</sup>, M.C. Gerstenberg<sup>c</sup>, B. Edinger<sup>a,b</sup>, B. Toperverg<sup>a,b</sup>, S.R. Forrest<sup>c</sup>, G. Scoles<sup>c</sup>, H. Dosch<sup>a,b</sup>

<sup>a</sup>Max-Planck-Institut für Metallforschung, Heisenbergstr.1, D-70569 Stuttgart, Germany

<sup>b</sup>Institut für Theoretische und Angewandte Physik, Universität stuttgart, Pfaffenwaldring 57, D-70550 Stuttgart, Germany

<sup>c</sup>Princeton Materials Institute, Princeton University, Princeton, NJ 08544, USA

## Abstract

An X-ray study of a crystalline organic–organic heterostructure, consisting of a film of PTCDA (3,4,9,10-perylenetetracarboxylic dianhydride) grown on a self-assembled monolayer (SAM) of decanethiol on Au(111), is presented. The sandwich structure acts as a “molecular interferometer”, where the interference between the Laue function of the PTCDA film and the crystal truncation rod (CTR) of the substrate is governed by the SAM spacer thickness,  $d_0$ . A pronounced destructive interference feature is observed, which allows the determination of  $d_0$  with great sensitivity. © 2000 Elsevier Science B.V. All rights reserved.

PACS: 61.66.Hq; 68.55.Gi

Keywords: Organic films; Surface scattering; Interference effects

## 1. Introduction

Thin films and multilayers of organic molecules are receiving considerable attention due to their exciting optical, optoelectronic, and electronic properties and their potential tunability. Several applications like organic light-emitting devices, solar cells, sensors, transistors, etc. have already been demonstrated [1]. However, compared to inorganic thin films, relatively little is known about the fundamental mechanisms governing the growth and structural phases of these materials and their relationship to electronic and optical characteristics. The different interactions (e.g., the greater importance of van-der-Waals forces for organic molecules) cause differences in the response to strain, in the epitaxy, and the thermal behavior, which makes a fundamental understanding of these issues mandatory for future progress.

As with inorganic systems, deposition in ultra-high vacuum (UHV) offers the chance to combine a clean environment and control of the growth on the sub-monolayer level with in situ analysis by a variety of surface science techniques. For these systems, questions related to growth and structure in the monolayer regime have been investigated to some extent, but less is known about the evolution of thicker films.

The understanding of crystalline organic–organic heterostructures is very limited due to the difficult preparation and applicability of only a restricted number of characterization techniques. Important questions in the context of these structures are, under which conditions a (single-) crystalline overlayer can be grown at all, if the structure can be described by an epitaxial relation, if the organic underlayer remains stable upon deposition of the organic adsorbate, and how stable the interface is against heating (thermal expansion, melting, interdiffusion, etc.).

In this paper, the structure and interface properties of an organic–organic heterostructure consisting of PTCDA (3,4,9,10-perylenetetracarboxylic dianhydride),

\* Corresponding author. Fax: (+ +49)-711-689-1902.

E-mail address: fschreib@dxray.mpi-stuttgart.mpg.de (F. Schreiber)

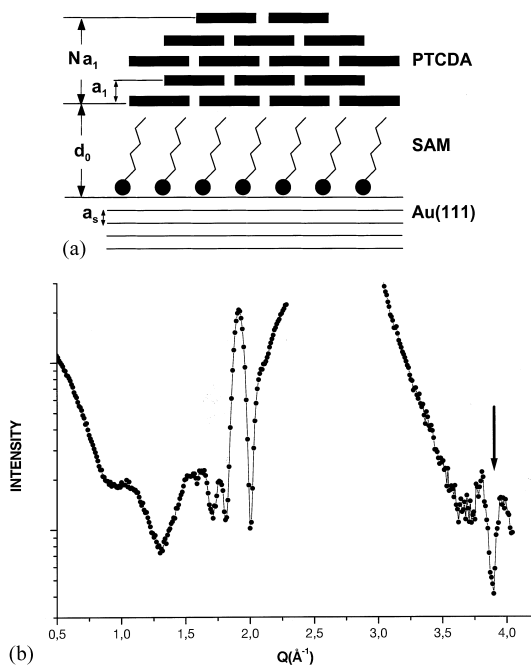


Fig. 1. (a) Schematic of the layered structure (PTCDA/SAM/Au(111) substrate). (b) Scan along the specular rod (data corrected for active area and Lorentz factor). Note the destructive interference feature (arrow) around the second-order Bragg peak of PTCDA ( $Q = 3.9 \text{ \AA}^{-1}$ ). Since the SAM spacer introduces an additional phase shift between the PTCDA and the substrate rod, their interference can be destructive, as seen from the fact that the signal of the entire sandwich structure on the substrate is *below* that of the interpolated substrate alone (see Fig. 2 for details).

a model compound for organic molecular beam epitaxy (OMBE) [1–5], grown on a self-assembled monolayer (SAM) of decanethiol on Au(111) [6] (see Fig. 1a for a schematic representation), are investigated by surface X-ray scattering techniques [7,8]. For such a complex structure as this PTCDA/SAM/Au(111) sandwich, not all issues can be discussed in one short paper. Here we focus on the interference effects between the different layers and the substrate and the understanding of the essential parameters. A more complete discussion of the structure including the (in-plane) epitaxy and strain can be found in Ref. [9].

## 2. Experiment

The experiments were performed at beamline X10B of the National Synchrotron Light Source at Brookhaven using a wavelength of  $\lambda = 1.13 \text{ \AA}$ . A small UHV chamber containing the single-crystal Au(111) substrate was mounted to a four-circle diffractometer. The chamber was equipped with a Be window, a sputter gun for in situ

cleaning, a leak-valve for dosing the decanethiol vapor, and a resistively heated custom-built Knudsen cell for deposition of PTCDA.

The Au(111) surface was prepared by repeated Ar sputter and anneal cycles until the  $23 \times \sqrt{3}$  reconstruction [10] characteristic of the clean Au(111) surface was seen and remained stable for at least 30 min. During growth, the substrate was kept at ambient temperature. The growth of decanethiol SAMs on Au(111) from the vapor phase had previously been studied in detail [11,12]. In the present study, the goal was simply to grow a SAM with full coverage (i.e., a complete monolayer with a  $c(4 \times 2)$  superlattice of the hexagonal ( $\sqrt{3} \times \sqrt{3}$ )R30° structure [13,14]). After completion of the SAM, PTCDA (typically about 20 monolayers) was evaporated from a Knudsen cell, similar as in a recent study of PTCDA on the bare Au(111) surface [3].

## 3. Results and discussion

### 3.1. In-plane structure

The structure of decanethiol SAMs had been studied by several groups [13,14]. For a full coverage SAM, a  $c(4 \times 2)$  superlattice of a hexagonal ( $\sqrt{3} \times \sqrt{3}$ )R30° structure is found. The hydrocarbon chains are tilted away from the surface normal by about 30°. Upon PTCDA deposition, the SAM structure remains unchanged, as evidenced by surface X-ray diffraction [9].

The PTCDA (102) peak (in bulk notation [5], corresponding to the stacking of flat-lying molecules) is aligned with the surface normal (see below). Also in-plane, well-defined peaks of PTCDA are found (azimuthally and radially) implying a well-defined crystallographic relationship between PTCDA and the methyl-terminated SAM surface, as opposed to powder rings due to azimuthally random orientation [9].

### 3.2. Out-of-plane structure

Scans along the specular rod show the rich interference features of this sandwich structure (Fig. 1). The overall shape is essentially determined by the CTR of the Au(111) substrate emanating from the bulk (111) Bragg peak at  $Q = 2\pi/a_s = 2.668 \text{ \AA}^{-1}$ . Superimposed on this are the interference fringes in the low- $Q$  regime with a relative spacing of  $\delta Q \sim 0.39 \text{ \AA}^{-1}$ , corresponding to a SAM spacer thickness  $d_0 \sim 16 \text{ \AA}$ , due to scattering from the top and bottom SAM interface. Furthermore, at  $Q = 2\pi/a_1 = 1.95 \text{ \AA}^{-1}$ , the (102) Bragg peak of PTCDA is found, indicating the expected planar stacking of the molecules along the surface normal [3]. Depending on the roughness, some Laue satellites of this peak can be observed.

The most striking feature is found at the second-order PTCDA Bragg peak, i.e., around  $Q = 2 \times 1.95 \text{ \AA}^{-1}$ . The total scattering intensity of the entire structure is significantly *lower* than that of the bare substrate (see Fig. 1b (arrow) and discussion below). This *destructive* interference of the PTCDA Bragg peak and the substrate rod is caused by the SAM, which acts as a spacer and introduces an additional phase shift ( $\sim e^{iQd_0}$ ) between the two scattering contributions [15,16].<sup>1</sup>

A complete model for all interference features of this heterostructure would obviously include a relatively large number of parameters and require a thorough discussion, which will be published elsewhere [17]. Here we want to limit ourselves to the destructive interference and show that this effect can be used for a very sensitive determination of the spacer thickness and possible changes of that. The total reflectivity on the specular rod is calculated from

$$\begin{aligned} |R_{\text{total}}|^2 &= |R_S + R_{\text{SAM}} + R_{\text{PTCDA}}|^2 \\ &= |R_S|^2 + |R_{\text{SAM}}|^2 + |R_{\text{PTCDA}}|^2 \\ &\quad + 2 \operatorname{Re}(R_S R_{\text{SAM}}^*) + 2 \operatorname{Re}(R_S R_{\text{PTCDA}}^*) \\ &\quad + 2 \operatorname{Re}(R_{\text{SAM}} R_{\text{PTCDA}}^*), \end{aligned} \quad (1)$$

where  $R_S$ ,  $R_{\text{SAM}}$ , and  $R_{\text{PTCDA}}$  are the reflectivity coefficients of the Au substrate, the SAM, and the PTCDA film, respectively. Briefly, the contribution from the PTCDA film is essentially a Laue function and can be written as

$$R_{\text{PTCDA}} = \frac{-iQ_c^2}{4Q} c_1 a_1 \tilde{F}_1(Q) \frac{\sin(NQa_1/2)}{\sin(Qa_1/2)} e^{iQa_1(N-1)/2} g_1(Q), \quad (2)$$

where  $N$  is the number of PTCDA out-of-plane lattice planes and  $a_1$  their spacing. The SAM is approximated as a slab of constant electron density, which leads to

$$R_{\text{SAM}} = \frac{-iQ_c^2}{4Q} 2c_0 \tilde{F}_0(Q) \frac{\sin(Qd_0/2)}{Q} e^{iQ(Na_1 + d_0/2)} g_0(Q). \quad (3)$$

The contribution from the Au substrate (CTR) with lattice spacing  $a_s$  is

$$\begin{aligned} R_S &= \frac{-iQ_c^2}{4Q} a_s \tilde{F}_s(Q) \frac{1}{2 \sin(Qa_s/2)} \\ &\quad \times (-i) e^{-iQa_s/2} e^{iQ(Na_1 + d_0)} g_s(Q). \end{aligned} \quad (4)$$

In these expressions,  $Q_c$  is the momentum transfer at the total reflection of the substrate. The  $c$ 's are the electron densities normalized to the substrate, the  $\tilde{F}(Q)$ 's are the normalized form factors, and the  $g(Q)$ 's comprise

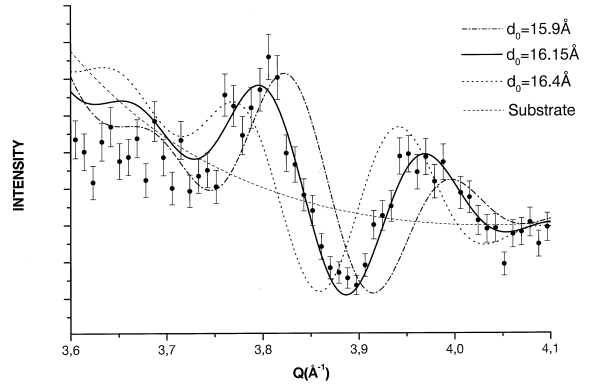


Fig. 2. Comparison of experimental data and simulations of the interference in the region of the second-order Bragg peak for different values of the spacer  $d_0$ . The sensitivity to small changes in  $d_0$  is demonstrated by the fact that already small changes in  $d_0$  lead to strong disagreement with the experimental data. Note that the total scattering of the heterostructure is below that of the substrate (broken line) around  $Q \sim 3.9 \text{ \AA}^{-1}$ .

attenuation terms due to roughness and Debye–Waller effect [17].

In the region of the second-order PTCDA Bragg peak, i.e. the destructive interference, the dominating contributions are from the substrate and the PTCDA film. The SAM introduces an additional relative phase shift  $\sim e^{iQd_0}$  between  $R_S$  and  $R_{\text{PTCDA}}$ , which causes the scattering of these terms to be out of phase. As indicated in Fig. 2, the total scattering of the heterostructure is below that of the substrate (broken line) around  $Q \sim 3.9 \text{ \AA}^{-1}$ . It is clear that the diffraction pattern responds sensitively to changes in  $d_0$ . In fact, as shown in Fig. 2, changing the spacer distance by only 0.25 Å in the simulations leads to an unacceptable fit, implying that changes on this scale can be readily detected.

We would like to point out that here at the second-order PTCDA Bragg peak,  $d_0$  refers to the distance between the lattice planes of PTCDA and the Au substrate. This includes the SAM thickness plus some contribution from the finite width of the substrate lattice planes and the PTCDA lattice planes, which can be roughly estimated as  $a_1/2 + a_s/2$ . For the purpose of using the destructive interference as a sensitive detector for small changes, however, this distinction between the SAM thickness itself and the distance between the lattice planes is irrelevant.

Furthermore, we note that for the observation of destructive interference it is favorable if the contributions  $R_S$  and  $R_{\text{PTCDA}}$  are of similar magnitude. This implies that for too thin or also too thick PTCDA films, it can become more difficult to observe the effect. Corresponding constraints apply to other factors that govern the magnitude of the respective scattering contributions, such as the roughness.

<sup>1</sup> Similar phase shift effects (but with a spacer of zero electron density) were discussed in Refs. [15,16].

In conclusion, the observation of the above interference effects demonstrates that this organic–organic heterostructure (PTCDA/SAM/Au(111)) can be grown with well-defined interfaces. Furthermore, due to the sensitivity to the parameters discussed, particularly the destructive interference can be used as a very sensitive indicator of small structural changes, which can be exploited, e.g., in temperature-dependent measurements [15].

### Acknowledgements

The authors wish to acknowledge the experimental assistance of T.Y.B. Leung and G. Bracco. The work was supported by the Deutsche Forschungsgemeinschaft (DFG), the Max-Planck-Gesellschaft, the Air Force Office of Scientific Research, and the Princeton MRSEC funded by the National Science Foundation. The X-ray measurements were performed at the NSLS (Brookhaven), which is supported by DOE Contract No. DE-AC0276CH-00016.

### References

- [1] S.R. Forrest, *Chem. Rev.* 97 (1998) 1793, and references therein.
- [2] E. Umbach, M. Sokolowski, R. Fink, *Appl. Phys. A* 63 (1996) 565.
- [3] P. Fenter, F. Schreiber, L. Zhou, P. Eisenberger, S.R. Forrest, *Phys. Rev. B* 56 (1997) 3046.
- [4] M. Möbus, N. Karl, *Thin Solid Films* 215 (1992) 213.
- [5] A.J. Lovinger, S.R. Forrest, M.L. Kaplan, P.H. Schmidt, T. Venkatesan, *J. Appl. Phys.* 55 (1984) 476.
- [6] A. Ulman, *An Introduction to Ultrathin Organic Films: From Langmuir-Blodgett to Self-Assembly*, Academic Press, Boston, 1991.
- [7] R. Feidenhans'l, *Surf. Sci. Rep.* 10 (1989) 105.
- [8] H. Dosch, *Critical Phenomena at Surfaces and Interfaces*, Springer Tracts in Modern Physics, Vol. 126, Springer, Berlin, 1992.
- [9] M.C. Gerstenberg, F. Schreiber, B. Toperverg, T.Y.B. Leung, G. Bracco, S.R. Forrest, G. Scoles, in preparation.
- [10] A.R. Sandy, S.G.J. Mochrie, D.M. Zehner, K.G. Huang, D. Gibbs, *Phys. Rev. B* 43 (1991) 4667.
- [11] F. Schreiber, A. Eberhardt, T.Y.B. Leung, P. Schwartz, S.M. Wetterer, D.J. Lavrich, L. Berman, P. Fenter, P. Eisenberger, G. Scoles, *Phys. Rev. B* 57 (1998) 12476.
- [12] P. Schwartz, F. Schreiber, P. Eisenberger, G. Scoles, *Surf. Sci.* 423 (1999) 208.
- [13] N. Camillone, C.E.D. Chidsey, G.-Y. Liu, G. Scoles, *J. Chem. Phys.* 98 (1993) 3503.
- [14] P. Fenter, A. Eberhardt, P. Eisenberger, *Science* 266 (1994) 1216.
- [15] I.K. Robinson, R.T. Tung, R. Feidenhans'l, *Phys. Rev. B* 38 (1988) 3622.
- [16] J. Falta, D. Bahr, A. Hille, G. Materlik, H.J. Osten, *Appl. Phys. Lett.* 71 (1997) 3525.
- [17] F. Schreiber, M.C. Gerstenberg, B. Edinger, B. Toperverg, S.R. Forrest, G. Scoles, H. Dosch, in preparation.